Journal of Coastal Research	10	2	329–338	Fort Lauderdale, Florida	Spring 1994

Estimation of Bottom Stress and Roughness in Lower Chesapeake Bay by the Inertial Dissipation Method†

J.P. Xu, L.D. Wright and J.D. Boon

Virginia Institute of Marine Science
School of Marine Science
College of William and Mary
Gloucester Point, VA 23062, U.S.A.

ABSTRACT

XU, J.P.; WRIGHT, L.D., and BOON, J.D., 1994. Estimation of bottom stress and roughness in lower Chesapeake Bay by the inertial dissipation method. *Journal of Coastal Research*, 10(2), 329–338. Fort Lauderdale (Florida), ISSN 0749-0208.

Shear velocities and associated hydraulic roughness lengths, z_0, and drag coefficients $C_D(100)$ were estimated for the bay-stem plains environment of lower Chesapeake Bay (depth 11–12 m) under calm conditions during winter. A modified inertial dissipation method was applied to field data obtained from an array of electromagnetic current meters supported by a bottom-mounted tripod. A wave-current boundary layer model (GRANT and MADSEN, 1986) was applied to the same set of data. The results show that when wave activity is minimal, the bed is dominated by biologic roughness with z_0 and $C_D(100)$ values of about 0.05 cm and 2.7×10^{-3} respectively.

ADDITIONAL INDEX WORDS: *Chesapeake Bay, estuaries, boundary layer, Kolmogorov spectrum, shear stress*

INTRODUCTION

Bottom shear stress integrates the flow dynamics and sediment dynamics and is thus crucial to understanding erosional and depositional changes of estuarine beds. This quantity determines both sediment suspension and flow structure in the boundary layer. Of the various methods that have been used to estimate the bottom shear stress, the two that are most feasible for field application are the mean flow method ("law of the wall") and the inertial dissipation method (HUNTLEY, 1988). The inertial dissipation method has been applied in estimations of bottom shear stress by several researchers. GRANT *et al.* (1984) successfully applied the method to CODE-II data and obtained shear stress estimates largely consistent with the results from the logarithmic profile method. HUNTLEY (1988) further suggested a modification that extends the conditions for the validity of the method. Our interest here lies in gaining a better understanding of the bottom drag that characterizes the floor of the bay-stem plains region of lower Chesapeake Bay (Figure 1). Secondarily, we are interested in ascertaining the applicability of the inertial dissipation method for estimating the temporal and spatial variability of bed stress in large estuaries.

92062 received 5 July 1992, accepted in revision 12 July 1993.
† Contribution No. 1803 from the Virginia Institute of Marine Science.

The purpose of this paper is to show the results of estimating the hydraulic roughness length of the bed of lower Chesapeake Bay using the inertial dissipation method. The shear velocity and roughness length resulting from available logarithmic profiles are compared to those obtained from the inertial dissipation method. Finally the results are used to verify the predicted values from the benthic boundary layer model of GRANT and MADSEN (1979, 1986).

BACKGROUND

The mean flow method involves estimating the bottom shear stress τ_0, from a mean flow profile within the lower part of turbulent boundary layers utilizing the Prandtl von Karman equation or "law of the wall"

$$\bar{u} = \frac{u_*}{\kappa} \ln\left(\frac{z}{z_0}\right) \qquad (1)$$

where u_* is the friction velocity defined as $u_* = (\tau_0/\rho)^{\frac{1}{2}}$, where τ_0 is bed shear stress, $\bar{u}$ is the time-averaged (typically over 10 minutes) flow velocity at elevation z, κ is von Karman's constant (about 0.4) and z_0 is the z intercept at which $\bar{u}$, notionally, becomes zero. The length z_0 thus expresses the hydraulic roughness of the bottom and is estimated by extrapolation of a log-normal velocity

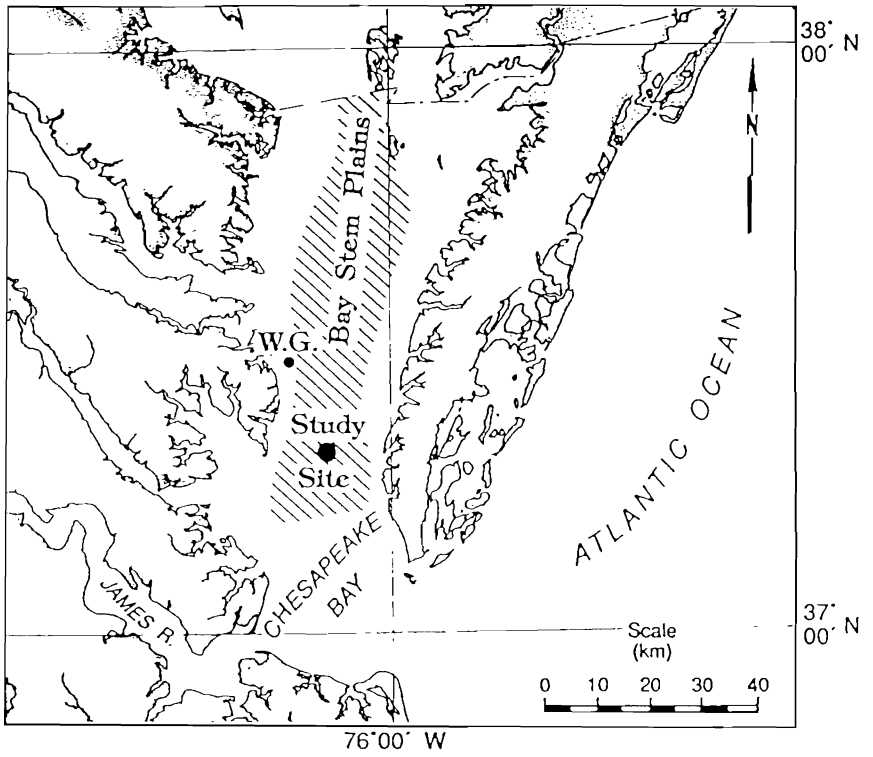

Figure 1. Study site location.

profile. To do this, simultaneous observations of u must be obtained from at least three and preferably four or five elevations and the resulting profile must be logarithmic. In addition to z_0, the elevation-dependent drag coefficient

$$C_D(z) = \left(\frac{u_*}{\bar{u}(z)}\right)^2 = \frac{\tau_0}{\rho \bar{u}^2(z)} = \left(\frac{\kappa}{\ln(z/z_0)}\right)^2 \quad (2)$$

affords a useful characterization of bottom drag.

Unlike the mean flow method, the inertial dissipation method requires only one flow meter at a specified distance above the bed and is thus attractive for studies of long-term temporal and spatial variability. The inertial dissipation method is based on the relationship between turbulent kinetic energy density and wave number in the inertial sub-range wherein the flux of energy from low to high wave numbers must be equal to the dissipation rate assuming that there are no local sources or sinks for the energy. The turbulent kinetic energy spectrum, S, is a function of wave number k and dissipation rate ϵ following

$$S = \alpha \epsilon^{2/3} k^{-5/3} \quad (3)$$

where α is the Kolmogorov constant, the value of which depends on which axis (longitudinal or vertical) the turbulent fluctuations are. This equation is usually called Kolmogorov's $k^{-5/3}$ law (KUNDU, 1990). Two assumptions must be made in order to relate Equation 3 to the bottom stress (HUNTLEY, 1988). First, a local balance is assumed to exist between the production and dissipation of turbulent energy. Second, it is essential that measurements are made within the constant stress part of the water column. The production of turbulent energy is

$$\left(\frac{\tau}{\rho}\right)\frac{\partial \bar{u}}{\partial z} = u_*^2 \frac{\partial \bar{u}}{\partial z} \quad (4)$$

and in the logarithmic layer, the "law of the wall" is described by

$$\frac{d\bar{u}}{dz} = \frac{u_*}{\kappa z}. \quad (5)$$

The assumption of a local balance between pro-

duction and dissipation rate of the turbulent energy, leads to

$$\varepsilon = \text{production} = \frac{u_*^3}{\kappa z}. \quad (6)$$

After substituting (6) into (3) and some manipulation, we get

$$u_* = \left[\frac{Sk^{\frac{3}{2}}}{\alpha}\right]^{\frac{1}{2}} (\kappa z)^{\frac{1}{2}}. \quad (7)$$

HUNTLEY (1988) pointed out that Equation 7 is not valid unless two conditions are satisfied. First, the measurements must be made within the constant stress layer. Second, a critical Reynolds number R_{ec}, which is usually taken as 3,000 to 4,000, must be exceeded to ensure separation between low wave number turbulence production and high wave number dissipation. By assuming that the second condition is generally satisfied, *i.e.*,

$$R_* = \frac{u_* \kappa z}{\nu} > R_{ec} \quad (8)$$

where ν is the kinematic viscosity of water, Equation 8 can be rewritten to give a critical height, z_{cr}, above which measurements must be made to ensure an inertial subrange:

$$z_{cr} = R_{ec}\nu/(\kappa u_*). \quad (9)$$

For low Reynolds number conditions in which z_{cr} could be above where measurements are made, HUNTLEY (1988) introduced a correction for the shear velocity

$$u_* = \left[\frac{\hat{u}_*^3 R_{ec}\nu}{(\kappa z)}\right]^{\frac{1}{4}} \text{ for } z < z_{cr} \quad (10)$$

where $\hat{u}_*$ is the value of shear velocity estimated from Equation 7 at height $z < z_{cr}$.

FIELD MEASUREMENTS

The field measurements on which this paper is based were obtained from the Wolf Trap bay-stem plains site in lower Chesapeake Bay (lat. 37° 16.33′ N, long. 76° 8.57′ W, Figure 1) over the late winter period 27 February to 5 March 1991 at a water depth of 11–12 meters. The benthic region of this site has been described in detail by WRIGHT *et al.* (1992). Typically, the mud bottom is fairly smooth with biogenic roughness (worm tubes, hummocks, and depressions) dominating micromorphology. Bottom sediment consists of 50% of very fine sand (0.10 mm) mixed with 35% silt and 15% clay. Although low amplitude waves commonly interact with tidal currents to enhance bed stress at this site (WRIGHT *et al.*, in press), wave agitation was conspicuously absent during the winter, 1991 observation period. In addition, biologic activity was probably at a minimum at this time so our observations are considered to characterize the smoothest extreme of bottom conditions.

The instrumented tripod (Figure 2) used to obtain the field measurements has been described in detail by WRIGHT (1989) and WRIGHT *et al.* (1992). This tripod supported a SeaData Model 635-9RS unit as well as a SeaData Model 626-3 current profiling system with three additional 2-axis electromagnetic Marsh-McBirney current sensors. The diameter of the spherical Marsh-McBirney sensors on the SeaData Model 626-3 and the single sensor on the Model 635-9RS unit is 3.8 cm. The four current sensors were mounted in a vertical array at elevations of 7.5, 37.1, 66.5 and 103.5 cm above the bed. The sensor at z = 37.1 cm was sampled at 5 Hz; the other three sensors were sampled at 1 Hz. Pressure was measured by a ParoScientific quartz pressure sensor mounted at 237.5 cm above the bed on the tripod. An Optical Backscattering Sensor array (including five sensors at 5.5, 11, 25.5, 49.5 and 96.7 cm above the bed, respectively) was also mounted on the tripod. A Digital Sonar Altimeter (DSA) mounted at 143.5 cm above the bed on the tripod was used to measure possible changes in the elevation.

The Marsh-McBirney current sensors were individually calibrated in steady flows before each field deployment using the VIMS 18 meter recirculating flume. Each axis of the spherical flow sensors was calibrated separately in both positive and negative directions. The frequency response of the current meter signal-processing electronics was measured by injecting a portion of the magnet-drive voltage multiplied by raised sinusoid signals covering a range of frequencies (0.1 to 10 Hz) into the receiver channel amplitude and phase (GREEN, *personal commuication*). The response thus measured was:

$$\Gamma(f) = \frac{1}{[1 + (m2\pi f)^2]^{\frac{1}{2}}} \quad (11)$$

where m = 0.09 for frequencies, f, out to 2.5 Hz, and the true spectrum is related to the measured spectrum by $S_{true}(f) = \Gamma^{-2} S_{meas}(f)$. All spectral

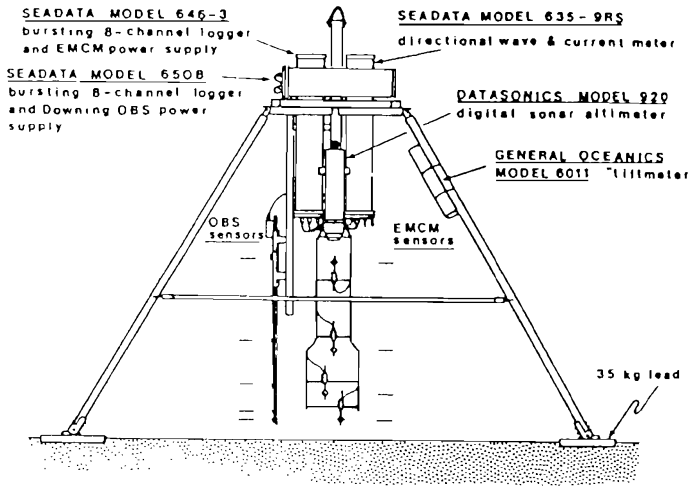

Figure 2. The VIMS benthic boundary layer tripod.

estimates reported here have been corrected for the measured frequency response of the current meter electronics.

Data loggers were synchronized and programmed for burst-mode sampling. The interval between bursts was two hours. There were 1,024 samples in each burst. Burst duration was 17 minutes for 626-3 unit, 3.5 minutes for 635-9RS unit and pressure sensor. The burst interval of the OBS sensors was 4 hours with a sample frequency of 1 Hz and a burst duration of 17 minutes.

ANALYSIS METHODS

Mean values from three of the four current sensors were used in applications of the mean flow method. Data from the uppermost sensor consistently showed unexpectedly low values, apparently as a result of partial sheltering by the tripod frame, and had to be discarded. Only the 5 Hz 635-9RS unit data sets were used in the inertial dissipation method since that is the only data with a Nyquist frequency high enough to embrace the inertial subrange. The time series velocity data (two horizontal components) were recorded on a Tattletale data logger in the field and then unpacked to diskette in the lab. Prior to spectral analysis, the two components were edited to remove unreasonable spikes. Following GWG, the data from each axis were then rotated into a stream-wise turbulent system (so that $\bar{v} = 0$)

$$\vec{u} = (\bar{u} + u', v') \tag{12}$$

where $\vec{v}$ is the current velocity vector, $\bar{u}$ is the downstream mean velocity, u' and v' are stream-wise and cross-stream fluctuating velocity components, respectively. The component u' was used in the spectral analysis.

Frequency spectra were calculated for each burst of 1,024 data points. The frequency spectra were then converted to wave number spectra. Following HUNTLEY and HAZEN (1988), Taylor's "frozen turbulence" concept was employed using:

$$S(k) = \frac{S(f)}{2\pi/\bar{u}} \tag{13}$$

where S(k) is the spectral density and a function of wave number k, S(f) is its counterpart in the frequency domain, f is frequency in Hz and $\bar{u}$ is the mean stream-wise velocity. According to TENNEKES and LUMLEY (1972), in order for Equation 13 to hold, we must have

$$\frac{kS(k)}{\bar{u}'} \ll 1. \tag{14}$$

For the Wolf Trap data discussed here, the inequality in Equation 14 was always satisfied.

NEAR-BOTTOM FLOWS

Time-series plots of burst-averaged current speed and direction together with the corresponding variations in tide height (water depth) for the first 72 hours of the deployment are shown in Figure 3. It is clear from Figure 3 that the currents

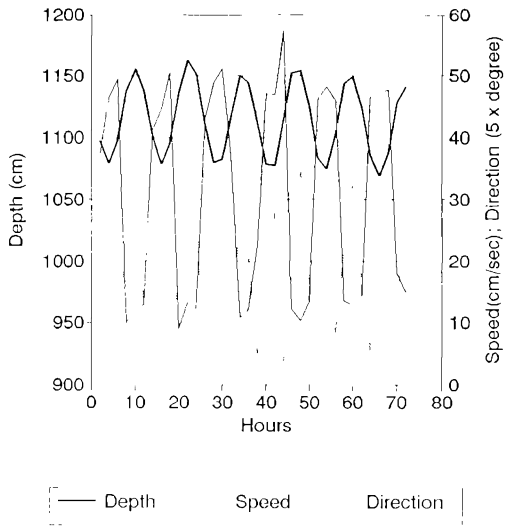

Figure 3. Time series of water depth, stream-wise current velocity and stream-wise current direction.

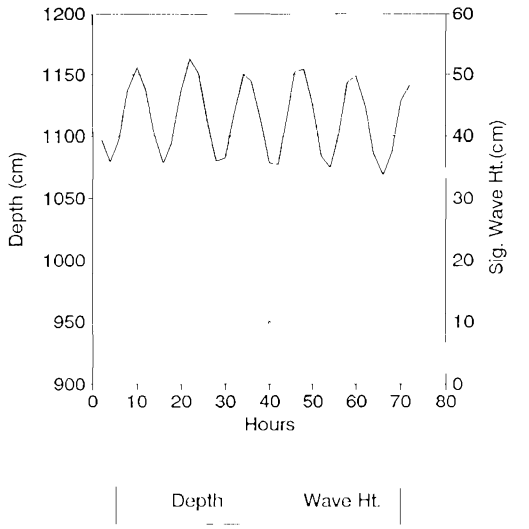

Figure 4. Time series of water depth and significant wave height.

during the experiment were tidally forced and relatively strong with speeds as high as 25–30 cm/sec at z = 40 cm. Significant wave heights for the same period are shown in Figure 4. Waves remained small (height < 15 cm) until the end of the period. The analyses presented here are only for the calm phase of the record.

Examples of within-burst time series of instantaneous (fluctuating) pressures and velocities of rotated stream-wise (u_{rot}) and cross-stream (V_{rot}) components of flow are shown in Figure 5 from which it is clear that waves were very small. The amplitude of fluctuation of rotated stream-wise velocities varied from burst to burst. For example, although the mean stream-wise velocities of the two bursts in Figure 5 were in the range of 10–15 cm/sec, the amplitude of the fluctuations were very different and bed stress must have also varied.

Three examples of mean current velocity profiles for which reasonably good logarithmic profiles were obtained are shown in Figure 6. From these profiles, u_* values ranging from 1.19–1.34 cm/sec and z_0 values of 0.004 cm–0.353 cm are obtained. The profiles also show that while the shear velocities don't vary much (three profiles are close to parallel), the hydraulic roughness lengths do. This may also indicate the primary effect of biologic activities on the bottom roughness. Sediment profiling camera images and plan-view photographs obtained by L.C. Schaffner (SCHAFFNER, 1990; SCHAFFNER and DIAZ, 1988) over several years show that species such as tube dwellers *Macrocylmene zonalis* and *Chaetopterus variopedatus*, the anemone *Ceriantheopsis americanus*, and numerous others contribute substantially to the bottom roughness. It has been indicated by SCHAFFNER (*personal communication*) that those species above normally adjust their activities and positions while the flow conditions vary. The organisms stretch out upward while the flow speed is small and shrink back at higher flow speed. When the organisms stretch out the roughness elements are high and eventually the hydraulic roughness computed from WOODING *et al.* (1973) and PAOLA (1985) will be high. At the time that organisms shrink back, the roughness is low. Figure 6 is a fairly good proof. The burst of highest flow speed has the lowest roughness length and the burst of lowest flow speed has the highest roughness length.

INERTIAL DISSIPATION ESTIMATES OF SHEAR VELOCITY

Of 36 bursts, 7 were found to satisfy Kolmogorov's $k^{-5/3}$ law. Figure 7 shows some of these wave number spectra along with a $-5/3$ slope line and their 95% confidence intervals.

In applying Equation 7 to calculate shear velocities, the lower wave number limit of the in-

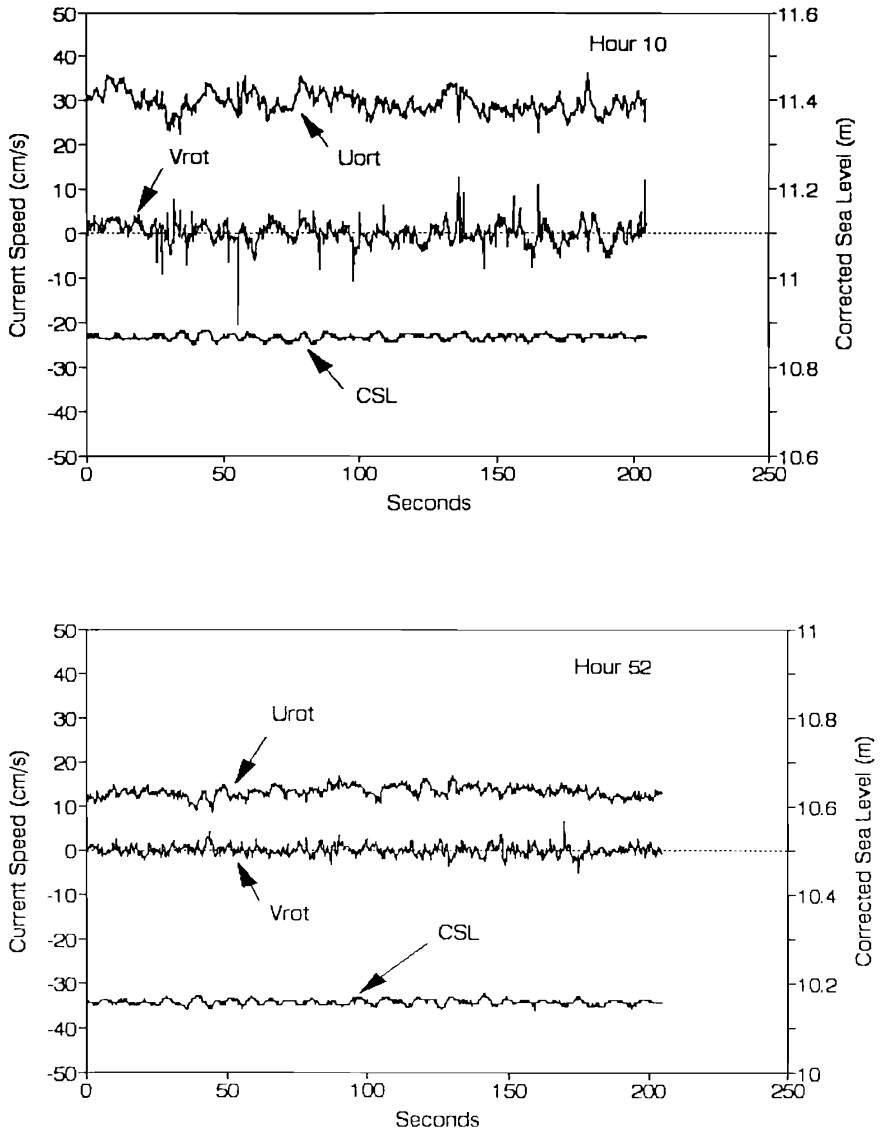

Figure 5. Plots of the time series of rotated velocities and water depth in selected bursts. u_{rot} = stream-wise speed, V_{rot} = cross-stream speed.

ertial subrange was chosen to be at or larger than twice the wave number of the expected turbulence peak (SOULSBY, 1983; GROSS and NOWELL, 1985). In our case, the flow sensor was at z = 37 cm and therefore the lower limit wave number was 0.17 rad./cm. The upper wave number limit for the subrange is set by the averaging volume of the response time of the flow sensors (HUNTLEY, 1988). According to GRANT and WILLIAM (1985), the upper wave number limit is that of an eddy twice the sensor size, and consequently equal π/L, where L is sensor length scale which in our case is 3.8 cm. So the upper wave number limit of the subrange is 0.83 rad/cm. In order to maximize confidence in the use of the calculated inertial subrange, we took the range to be from 0.24–0.67 rad./cm.

The second step in the analysis is to obtain a

Table 1. *Estimated shear velocity, roughness and drag coefficient.*

Hours	U_*	Z_0	k_b	C_D
10	1.6822	0.0336	1.0074	0.0025
22	1.6698	0.0220	0.6597	0.0023
36	1.4118	0.0846	2.5391	0.0032
46	1.4873	0.0401	1.2016	0.0026
48	1.9823	0.0343	1.0294	0.0025
58	1.4008	0.0730	2.1904	0.0031
72	1.5270	0.0439	1.3163	0.0027
Mean		0.0431	1.2922	0.0027

regression line using the data points within the inertial subrange in order to confirm that the slope is really close to $-5/3$. Finally, the lower and upper limits and the middle point of the wave number and their corresponding spectral density values are used as input to calculate the shear velocity value by Equation 7. The shear velocity value is corrected by Equation 10 when necessary.

Table 1 suggests that under the calm winter conditions that our measurements were made, the bed is hydraulically smooth with k_b being typically around 1 to 2 cm. The corresponding $C_D(100)$ averaged 2.7×10^{-3}, these values were less than the wave-enhanced values of $3.5–5.5 \times 10^{-3}$ estimated from 1987 and 1988 data obtained during times of moderate wave activities (WRIGHT *et al.*, in press). Even wouthout wave effects, the estimated biological roughness, k_{bio}, as calculated from the empirical formula of WOODING *et al.* (1973) and PAOLA (1985) utilizing observed dimensions of biologic roughness elements (during spring and summer) should be in the neighborhood of 2 cm (with a corresponding z_0 of 0.067 cm, WRIGHT *et al.*, in press). Presumably, the smoother conditions summarized in Table 1 attest to the reduced biologic activity of late winter in additon to minimal wave activity.

ESTIMATION OF AVERAGE ROUGHNESS

The bottom roughness of those 7 bursts are obtained and then compared with the input biogenic roughness of the GRANT and MADSEN (1986) model. By substituting the measured values of u_* and $\bar{u}$ into Equation 1, we can solve for z_0. The roughness lengths so obtained are listed in Table 1 which shows that large scatter exists. The large scatter of the z_0 values suggests that errors may result from this approach partially because z_0 is very sensitive to shear velocity u_* because of the exponential relationship. Thus, it is best to obtain

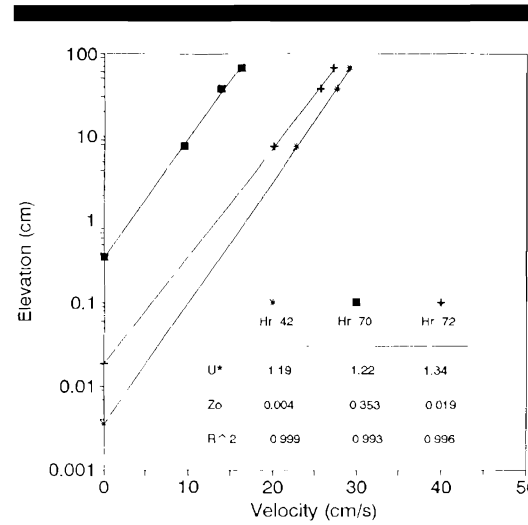

Figure 6. Some logarithmic velocity profiles and their corresponding shear velocities, physical roughness and regression coefficient.

the mean roughness value by converting the values of z_0 to their natural logarithmic counterparts whose average is then taken exponential to obtain the mean roughness length scale z_0. The averages of z_0, k_b and drag coefficient C_D are also listed in Table 1. Even though the estimated hydraulic roughness length z_0 at hour 72 (which is the only burst having both reasonable logarithm profile and $-5/3$ slope in spectrum) from mean flow method and inertial dissipation method are almost two times different, both mean z_0 and mean k_b (0.0431 cm, 1.2922 cm, respectively) calculated from the above method are close to the GRANT and MADSEN (1986) model input roughness which gives more practical shear velocities (Figure 8). Additionally, these values are comparable to the values estimated by means of the methods of WOODING *et al.* (1973), PAOLA (1985), WRIGHT *et al.* (in press). Since the inertial dissipation method of estimating shear velocity is not very accurate and includes errors resulting from the deviation of the regression line slope from the $-5/3$ on which the method is based, it is better to average the natural logarithmic values in order to reduce the sensitivity of roughness to the shear velocities.

COMPARISON WITH PREDICTION BY A BOUNDARY LAYER MODEL

Among several bottom boundary layer models, that of GRANT and MADSEN (1979, 1986) is widely

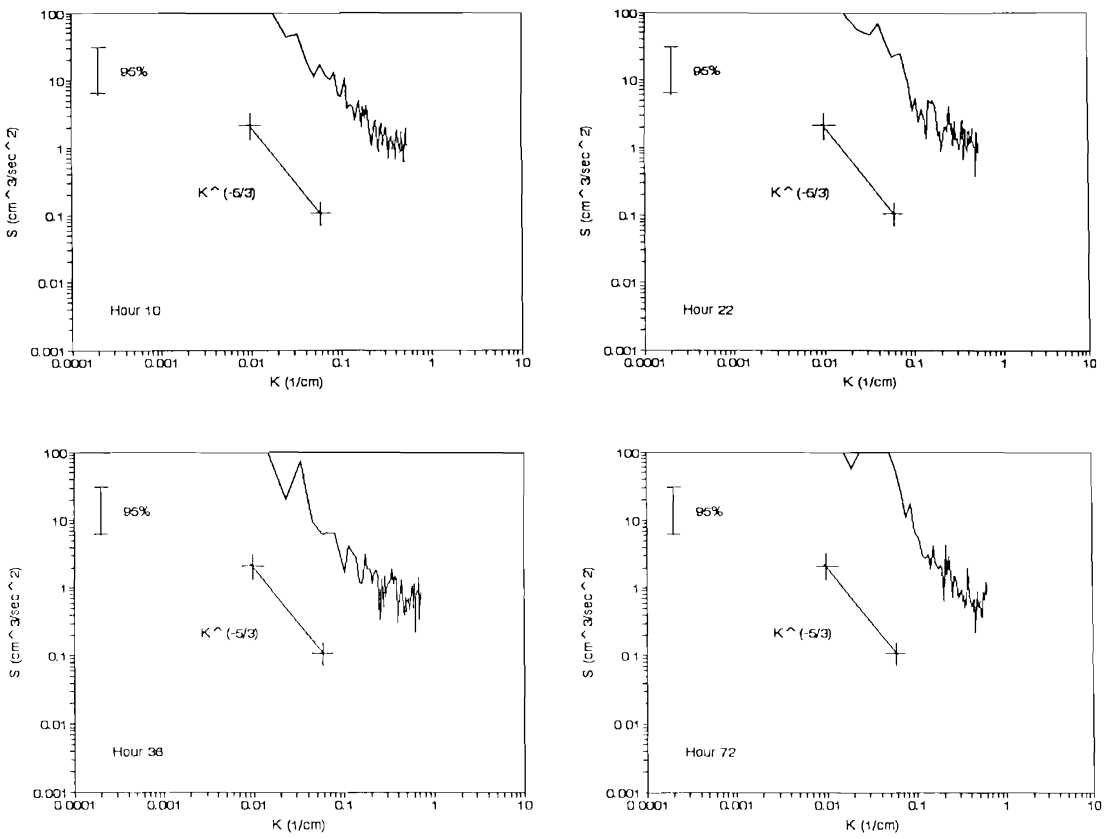

Figure 7. Plots of wave number spectra of 4 selected bursts.

accepted. The procedures for predicting the shear velocity in boundary layers affected by waves and currents have been described in detail (GRANT and MADSEN, 1979, 1982, 1986). We apply an algorithm to calculate the shear velocity using the same time series used in the inertial dissipation method. The input to the model includes water depth, significant wave height, significant wave period, mean current speed at the sensor height (37 cm in this case), and angle between wave propagation and current. Sediment diameter is also a parameter for input. We chose a constant input sediment size of 0.13 mm which is the mean grain size at Wolf Trap site. One important step in the

Table 2. *Predicted and estimated shear velocities.*

Hours	Predicted						Estimated
	$k_{bc} = 0.1$	$k_{bc} = 0.5$	$k_{bc} = 1$	$k_{bc} = 2$	$k_{bc} = 3$	$k_{bc} = 5$	
10	1.2817	1.5377	1.6882	1.8725	2.0006	2.1884	1.6822
22	1.3602	1.6330	1.7934	1.9900	2.1257	2.3260	1.6698
36	0.9573	1.1510	1.2651	1.4047	1.5009	1.6420	1.4118
46	1.1412	1.3788	1.5205	1.6961	1.8186	1.9970	1.4873
48	1.5345	1.8436	2.0256	2.2488	2.4038	2.6312	1.9823
58	0.9576	1.1505	1.2635	1.4024	1.4987	1.6393	1.4008
72	1.3048	1.6110	1.8025	2.0487	2.2238	2.4803	1.5270

Grant and Madsen model is to calculate the total bottom roughness, which consists of the grain roughness, wave or current induced ripple roughness (distributed roughness) and sediment transport roughness (GRANT and MADSEN, 1979, 1982, 1986). Since the waves were very weak during the observation period, neither ripple roughness nor sediment transport roughness were important. The biogenic roughness caused by the benthic organism activities was probably dominant in our case.

The GRANT and MADSEN (1986) model was run for the 7 sets of data which gave reasonable $-5/3$ slope during the spectral analysis using different values of biologic roughness, k_{bio}. Table 2 summarizes the results. The predicted shear velocities by GRANT and MADSEN (1986) model and estimated shear velocities by inertial dissipation method are plotted in Figure 8. Considerable scatter exists. Discrepancies between estimated and predicted shear velocities probably results largely from uncertainties concerning biologic roughness. The parameters used in Wooding and Paola's equation to calculate the biogenic roughness are obtained from bottom photographs. When using this method, large errors occur in estimating the height, spacing and the areal concentration of roughness elements. It is seen from Figure 8 that the predicted shear velocities are much closer to the estimates when biologic roughness k_{bio} is set to 1 cm.

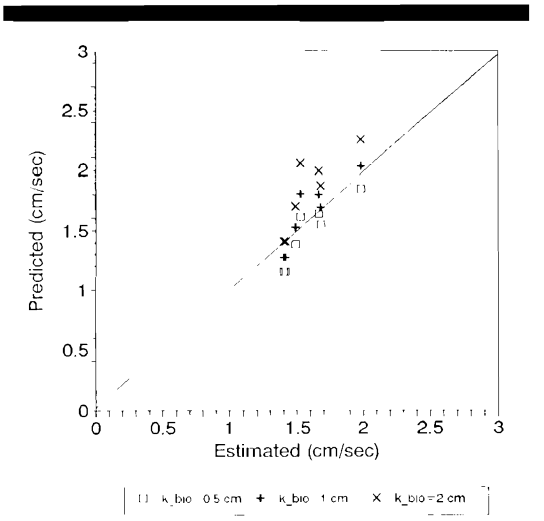

Figure 8. Comparison of estimated and predicted shear velocities.

CONCLUSIONS

From the foregoing, it can be cautiously concluded that reasonable agreement is obtained for the shear velocities estimated by the inertial dissipation method and the Grant and Madsen boundary layer model. The estimated bottom roughnesses are on the order of 1.5 cm which agrees roughly with the value calculated from WOODING *et al.* (1973) and PAOLA's (1985) (WRIGHT *et al.*, in press) equation. Since there is only one burst (hour 72) which satisfies the conditions of "law of the wall" and the Kolmogorov's "$-5/3$ law", no reasonable comparison between estimated values from the two methods can be made. Because waves are almost negligible during the observation period, shear velocities were dependent solely on mean (tidal) current velocity and bed micromorphology. Using the bottom roughness as the input parameter of the GRANT and MADSEN (1986) model, we found that the predicted shear velocities agree well with those estimated from the inertial dissipation method. This suggests that the GRANT and MADSEN (1986) model is still applicable to a current dominated estuarine system.

ACKNOWLEDGEMENTS

This study has been supported by the Chesapeake Bay Environmental Effects Committee/Toxics Research Program *via* the Virginia Graduate Marine Science Consortium project number R/CBT-4. The authors are grateful to R.A. Gammisch, F.H. Farmer and D. Hepworth for technical support. We thank Dr. O.S. Madsen and Dr. M.O. Green for their valuable discussion during the study. L.T. Marshall typed and proofread the manuscript.

LITERATURE CITED

GRANT, W.D. and MADSEN, O.S., 1979. Combined wave and current interaction with a rough bottom. *Journal of Geophysical Research*, 84, 1797–1808.

GRANT, W.D. and MADSEN, O.S., 1982. Movable bed roughness in oscillatory flow. *Journal of Geophysical Research*, 87, 469–481.

GRANT, W.D. and MADSEN, O.S., 1986. The continental shelf bottom boundary layer. *Annual Review of Fluid Mechanics*, 18, 265–305.

GRANT, W.D. and WILLIAM, A.J., 1985. Reply (to Gust). *Journal of Physical Oceanography*, 15, 1238–1243.

GRANT, W.D.; WILLIAM, A.J., and GLENN, S.M., 1984. Bottom stress estimates and their prediction on the northern Californian continental shelf during CODE-1: The importance of wave-current interactions. *Journal of Physical Oceanography*, 14, 506–527.

GROSS, T.F. and NOWELL, A.R.M., 1985. Spectral scaling

in a tidal boundary layer. *Journal of Physical Oceanography*, 15, 496–508.

HUNTLEY, D.A., 1988. A modified inertial dissipation method for estimating seabed stresses at low Reynolds numbers, with application to wave/current boundary layer measurements. *Journal of Physical Oceanography*, 18, 339–346.

HUNTLEY, D.A. and HAZEN, D.G., 1988. Seabed stresses in combined wave and steady flow conditions on the Nova Scotia continental shelf, field measurements and predictions. *Journal of Physical Oceanography*, 18, 347–362.

KUNDU, P.K., 1990. *Fluid Mechanics*. Academic Press, 638p.

PAOLA, C., 1985. A method for spatially averaging small-scale bottom roughness. *In:* NOWELL, A.R.M. and HOLLISTER, C.D. (eds.), *Deep Ocean Sediment Transport—Preliminary Results of the High Energy Benthic Boundary Layer Experiment. Marine Geology*, 66, 291–301.

SCHAFFNER, L.C. 1990. Small-scale organism distributions and patterns of species diversity: Evidence for positive interactions in an estuarine benthic community. *Marine Ecology Progress Series*, (in press).

SCHAFFNER, L.C. and DIAZ, R.J., 1988. Abundance and distribution patterns of the blue crab, *Callinectes sapidus*, in the lower Chesapeake Bay during the winter 1985–86. *Estuaries*, 11, 68–72.

SMITH, J.D., 1977. Modeling of sediment transport in continental shelves. *In:* GOLDBERG, E.D. (ed.), *The Sea 6*. John Wiley, pp. 539–577.

SOULSBY, R.L., 1983. The bottom boundary layer of shelf seas. *In:* JOHNS, B. (ed.), *Physical Oceanography of Coastal and Shelf Seas*. Elsevier, pp. 189–266.

TENNEKES, H. and LUMLEY, J.L., 1972. *A First Course in Turbulence*. MIT Press, 300p.

WOODING, R.A.; BRADELEY, E.F., and MARSHALL, J.K., 1973. Drag due to regular arrays of roughness elements of varying geometry. *Boundary-Layer Meteorology*, 5, 285–308.

WRIGHT, L.D., 1989. Benthic boundary layers of estuarine and coastal environments. *Reviews in Aquatic Sciences*, 1, 75–95.

WRIGHT, L.D.; BOON, J.D.; XU, J.P., and KIM, S.C., 1992. The bottom boundary layer of the bay stem plains environment of lower Chesapeake Bay. *Estuarine, Coastal and Shelf Science*, 35, 17–36.